Molecular Level Interface Designs Using Self-Assembling Technique for Stabilizing Langmuir-Blodgett Films

Zhong-Fan Liu*), Chun-Xia Zhao, Jin Zhang, Ming Tang, Tao Zhu and Sheng-Min Cai

Center for Intelligent Materials Research (CIMR), College of Chemistry and Molecular Engineering, Peking University, Beijing 100871, China

Key Words: Atomic Force Microscopy / Azobene / Electrochemistry / Interfaces / SAM-LB / Spectroscopy, Infrared / Surface / RA-FTIR

Self-assembled monolayers (SAMs) of HS-$(CH_2)_2$-X with X being -COOH, -OH, $-NH_2$, and $-CH_2SO_3Na$ were fabricated on Au surfaces for deposition of C_8H_{17}-C_6H_4-N=N-C_6H_4-O-$(CH_2)_3$-COOH (ABD) LB films. Thus-created SAM/LB interfaces were studied by the grazing-angle incident reflection absorption FTIR technique. For $-NH_2$ group, the interface was proved to be dominated by $-NH_3^+$ $^-$OOC- ionic bonding structure. When X was -COOH, an eight-membered face-to-face hydrogen bond was observed at the SAM/LB interface. With the -OH terminated interface, two types of hydrogen bond were created: one is the face-to-face hydrogen bond and the other one is the side-by-side hydrogen bond. In the case of Au/$-CH_2SO_3Na$/HOOC- interface, two terminal groups seem to exchange their cations, forming a $-CH_2SO_3H$/NaOOC-structure. The stability of these monolayer assemblies was investigated using Atomic Force Microscopy (AFM). It is found that all these films showed a greatly improved structural stability and the destructive three-dimensional rearrangement of ABD molecules has been effectively prohibited. The sequence of film stability was $-NH_2$ > -COOH > -OH > $-CH_2SO_3Na$, with the first two interfaces exhibiting even nice stability in aqueous solution, strong enough for tolerating the interfacial electron transfer studies.

Introduction

Monolayer assemblies such as Langmuir-Blodgett (LB) films and self-assembled monolayers (SAMs) have received a great deal of interests in the last decade because of their fascinating potential applications [1 – 3]. We have been paying particular and continuous attention to the azobenzene-functionalized monolayer assemblies. Azobenzene chromophore is photochemically reactive, originating from its reversible trans-cis photoisomerization, and is also electrochemically reactive owing to its red-oxidation. This makes azobenzene system rich of possibilities for various technological and fundamental studies. Up to now, we have extensively studied the physicochemical properties of azobenzene SAMs and LB films, which covered the photochromism [4, 5], the long-range electron-transfer kinetics [6 – 12], the memory phenomenon [13], the actinometric property [14, 15], the inversion phenomenon [16], the novel electrostatic isomerism phenomenon [17], and the thermal isomerization kinetics [18]. It should be noted that C.A. Mirkin and his colleagues have also conducted a number of original work on azobenzene SAMs recently [19 – 21]. They have paid special attention on the electrochemical properties of azobenzene-functionalized SAMs and the structural characterization using synchrotron in-plane X-ray diffraction, atomic force microscopy, and surface-enhanced Raman spectroscopy. For electrochemical and photoelectrochemical studies, the azobenzene LB films are generally deposited onto conductive and transparent SnO_2 glasses or gold-evaporated glasses. One of the troublesome problems often encountered in the experiments is the instability of the highly-organized LB film structures. Rearrangement of molecules on the supporting substrate surface frequently occurs because of the weak interaction between the LB films and the substrates, which leads to the collapse of ordered film structure and/or simple peeling off of the LB film into the adjacent solution. Although the structural stability has been greatly improved in azobenzene SAMs where molecules are nearly covalently bound to the substrate surface via, for example, Au-S bonding [8, 10, 11], the azobenzene chromophores are usually very closely packed and there is not enough free space in such SAMs allowing the photochemical isomerization, which is known to be accompanied by a remarkable molecular structure change [4, 22].

Self-assembling technique provides a simple but effective way to make a molecular level design of surface [1]. By selecting an appropriate terminating functional group, specific intermolecular interaction would be created between the SAM-modified substrate and the deposited LB film. In this paper, we demonstrate that such enhanced interactions will effectively improve the structural stability of LB films. Unlike highly packed azobenzene SAMs, such SAM/LB composite films may also have some degree of freedom to maintain both photochemical and electrochemical reactivities of azobenzene chromophore. As a subject for investigation, four different thiol compounds, HS-$(CH_2)_2$-X (X = -COOH, -OH, $-NH_2$, and $-CH_2SO_3Na$, respectively) were chosen to modify the Au surface before deposition of a model compound, C_8H_{17}-C_6H_4-N=N-C_6H_4-O-$(CH_2)_3$-COOH (ABD) LB film (see Fig. 1 in detail). The terminal groups X of these compounds, which are facing to the LB monolayer, will provide different types of interactions with the carboxyl group of the model compound, such as ionic bonding or hydrogen bonding, etc. We will show that the homogeneity and stability of LB films are strongly dependent on the interfacial bonding characteristics between the SAM and the LB film. We employed the atomic force microscopy (AFM) to obtain the morphological information of the LB film and the direct

*) Author to whom correspondence should be addressed:
Tel. and Fax: 86-10-6275-7157.
E-mail: lzf@chemms.chem.pku.edu.cn

  0005-9021/97/0808-1113 $ 15.00+.25/0

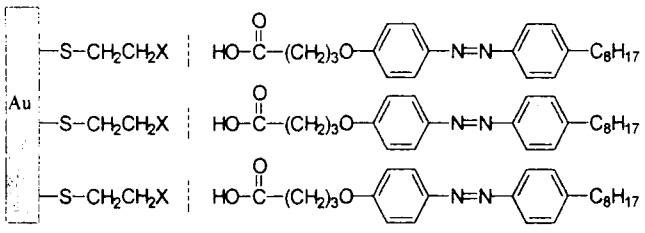

Fig. 1
Schematic illustration of the SAM/LB composite monolayer assembly. The Au surface was first modified by a thiol SAM terminated by -COOH, -OH, $-NH_2$ and $-CH_2SO_3Na$, respectively, and then the ABD monolayer was deposited on it using LB technique

evidence of the stabilizing effect. We also used the grazing-angle incident reflection absorption FTIR (referred to as RA-FTIR) technique in order to understand the bonding nature at the SAM/LB interface.

Experimental Section

Materials

4-Octyl-4′-(3-carboxy-trimethylene-oxy)-azobenzene (referred to as ABD) and β-mercaptopropionic acid (MPA) were purchased from Dojindo Laboratory (Kumamoto, Japan). 2-Amino-ethanethiol (AET) was obtained from Tokyo Kasei (TCI, Tokyo), 2-mercaptoethanol (ME) was from Beijing Hongxing Biochemicals, and 3-mercapto-1-propanesulfonic acid, sodium salt (MPS) was from Aldrich. All these chemicals were of reagent grade and used without further purification.

Preparing SAM-Modified Substrates

Gold substrates were prepared by vacuum evaporation of 200 nm thick gold on mica for AFM studies or on glass slides for RA-FTIR studies. To improve the adhesion of gold to the substrate, glass slides or mica had been precoated with 10 nm of chromium. Before use, thus-prepared gold substrates were cleaned in hot *piranha solution* (a hot solution of 30% H_2O_2 and 70% concentrated H_2SO_4 in volume ratio) followed by rinsing with milli-Q water and absolute ethanol. The SAMs were then fabricated by immersing the Au substrate into an ethanol solution of each thiol compound for 24 h. Upon removal from the solution, the substrates were extensively rinsed with absolute ethanol and then water.

LB Film Deposition

The ABD monolayers in its trans form were deposited onto the SAMs-modified substrate surfaces by a commercialized Langmuir trough (FACE, Japan). A milli-Q water (>17 MΩ cm) was used as the subphase and chloroform was used as the spreading solvent of ABD. The ABD monolayers were transferred to the solid substrates by vertical dipping at a rate of 10 mm/min. The transfer ratio falls into a range of 0.9 – 1.1 throughout the experiments. Because of the nice hydrophilicity of the SAMs-modified substrates, only one monolayer of ABD was deposited onto the substrate surface during the dipping and raising processes, with the hydrophilic carboxylic acid group of ABD facing to the SAMs. The surface pressure was kept at 20 mN/m, and the subphase temperature was controlled at 20 °C by a thermostat (UC-55, Tokyo Rikakikai).

Infrared Spectroscopy

Infrared spectra were obtained with a Perkin-Elmer System 2000 FTIR spectrometer equipped with a DTGS detector. A SPECAC variable angle reflection attachment was used for reflection absorption measurements and at an incidence angle of 82° (near grazing angle). All the spectra were obtained by referencing 1000 sample scans to 1000 bare gold background scans at 4 cm^{-1} resolution with strong apodization. The sample chamber was purged with dry N_2 to eliminate the spectral interference of water vapor in air.

AFM Imaging

AFM images were taken with a Nanoscope III (Digital Instruments (DI), Santa Barbara, CA) in a contact mode. The AFM cantilever was also purchased from the DI company (Integral Si_3N_4 nanoprobes, 200 μm leg). The force between the AFM tip and the sample was kept constant during scanning and the typical value used was ca. 2 nN. All the measurements were performed at the laboratory ambient.

Electrochemical Measurements

Electrochemical experiments were conducted in a single compartment, three-electrode cell, which has a small quartz window for introducing the irradiation light. The modified Au substrate was used as a working electrode. An Ag/AgCl, saturated KCl and a Pt wire were employed as the reference and counter electrodes, respectively. Cyclic voltammograms (CVs) of the composite films were obtained with a Hokuto Denko HA-150 potentiostat paired with a HB-111 function generator. The signals were recorded on a Riken Denshi F-35A X-Y recorder. All the CVs were taken in 0.1 M aqueous sodium perchlorate solution buffered with *Britton-Robinson* method, which was freed from oxygen by bubbling with nitrogen.

The photochemical trans-cis isomerization of ABD molecules in the composite films was induced by using a 500 W xenon lamp (Ushio Electric, UI-501C, Japan). The excitation wavelength was isolated with a suitable glass filter (Kenko, U-360 bandpass filter for UV output and cut-off filter at 440 nm for visible output).

Contact-Angle Measurements

Contact-angle experiments were performed with a contact-angle goniometer (Model JJC-2, The Fifth Optical Instrument Factory of Chang-chun) under ambient conditions

(15 – 20°C 50 – 60% relative humidity) using yellow light to illuminate the water droplet. The advancing contact angle was obtained by expanding a water droplet from a microsyringe until it advances smoothly across the surface and then measurement was made within 10 – 20 s after expansion. Each given value represents an average of at least four measurements.

Results and Discussion

A. General Observation

To obtain the structural information of ABD LB monolayer on different SAM-modified gold surfaces, Fourier transform infrared-spectroscopic measurements were made in the grazing-angle incident reflection absorption mode (RA-FTIR). For simplicity, the ABD monolayer assemblies on different substrates were abbreviated as Au/HOOC- (on naked gold), Au/-COOH/HOOC-, Au/-OH/HOOC-, Au/-NH_2/HOOC- and Au/-CH_2SO_3Na/HOOC- in the following description. Fig. 2 shows the RA-FTIR spectra of these assemblies, which correspond to two spectral regions, 3000 – 2800 cm^{-1} and 1800 – 800 cm^{-1}, respectively. Band assignments and peak positions are given in Table 1 [33, 39, 40].

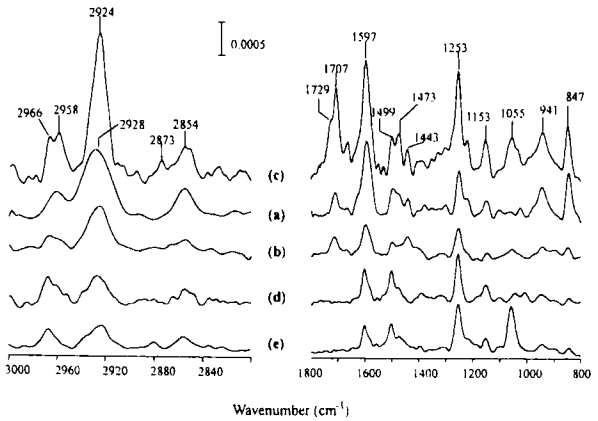

Fig. 2
RA-FTIR spectra of ABD LB monolayer on differently-modified gold substrates. (a) On naked Au (referred to as Au/HOOC- in the text); (b) Au/-COOH/HOOC-; (c) Au/-OH/HOOC-; (d) Au/-NH_2/HOOC-; (e) Au/-CH_2SO_3Na/HOOC-

The presence of ABD monolayer on gold surface is clearly evidenced by a series of characteristic vibration bands shown in the spectra. For instance, in the case of Au/-OH/HOOC- (see Fig. 2c), the absorption band appeared at 1707 cm^{-1} is assigned to the carbonyl stretching mode of carboxylic acid group, the bands at 1597, 1499 and 1473 cm^{-1} are to the in-plane vibration bands of benzene ring, and the bands at 1253, 1153, 1055, 941 and 847 cm^{-1} are attributed to the ϕ-O stretching band, ϕ-N stretching band, O-R stretching band, the OH···O in-plane bending stretching of -COOH, and out-of-plane bending band of ϕ-H, respectively. In the higher frequency region, the C-H stretching vibration bands were also observed clearly. The bands at 2966 and 2958 cm^{-1} can be assigned to the CH_3 asymmetric in-plane stretching mode and the asymmetric out-of-plane stretching mode, and the bands at 2924 and 2854 cm^{-1} to the CH_2 asymmetric and symmetric modes, respectively. Previous reports [41, 42] have shown that the absorption of alkanethiol SAMs with very short chain length was very weak. So these strong peaks should be mainly attributed to the C-H vibration of ABD molecules. For the other three SAMs-modified surfaces, some peaks disappeared, such as the C=O stretching mode around 1710 cm^{-1} in Au/-NH_2/HOOC- and in Au/-CH_2SO_3Na/HOOC-, and some new absorption peaks appeared, depending on the bonding nature at the SAM/LB interfaces.

B. SAM/LB Interfacial Structures

Close examination of the infrared spectra in Fig. 2 provides insight into the intermolecular interaction and thus the bonding character at the SAM/LB interface. In the following, we will give the respective description of each specifically-designed interface.

B(1). Au/HOOC-

Bare gold substrates prepared by vacuum evaporation showed a relatively poor hydrophilic property. The advanc-

Table 1
Observed bands and their assignments of ABD LB monolayer deposited on bare gold and four kinds of SAMs-modified gold substrates

Mode description	Au/-COOH	Au/-NH_2/HOOC-	Au/-COOH/HOOC-	Au/-OH/HOOC-	Au/-CH_2SO_3Na/HOOC-
$\nu_a(CH_3)$	2960	2967	2966	2966	2967
$\nu_a(CH_2)$	2928	2926	2925	2924	2923
$\nu_s(CH_3)$	–	2880	2880	2873	2880
$\nu_s(CH_2)$	2855	2855	2854	2854	2856
ν(C=O)	1713	–	1713	1729, 1707	–
Benzene ring	1596, 1498, 1470	1602, 1501, 1475	1598, 1498	1597, 1499, 1473	1601, 1501, 1476
$\nu_a(COO^-)$	–	1552(W)	–	–	1552(W)
$\nu_s(COO^-)$	–	1390	–	–	1393
ν(ϕ-O)	1252	1254	1253	1253	1253
ν(ϕ-N)	1151	1152	1147	1153	1152
ν(O-R)	1056(W)	1053	1054	1055	1058
δ(OH···O)	946	947	943	941	943
δ(ϕ-H)	846	843	846	847	843

ing contact angle of water droplet was ca. 40 – 60°, which depended sensitively on the pretreating condition of substrate and its exposure to air. The ABD LB monolayer on it was extremely instable, as directly evidenced by the AFM data shown in Fig. 3a, obtained one day after deposition. The white spots represent the aggregated ABD molecules, which were never observed on the naked gold surface.

The structural instability of ABD monolayer on naked gold has also been convinced by the RA-FTIR data shown in Fig. 2a. The peak at 1713 cm^{-1} is assigned to the carbonyl stretching mode characteristic of a carboxylic acid in a hydrogen-bonding environment, as noted in several published works [23 – 30]. We did not find any discernible absorption band around 1740 cm^{-1}, which is typical for carbonyl stretching of the unassociated carboxylic acid and is usually taken as an indicator of the presence of free carboxylic acid group in monolayer assemblies [24]. Therefore all the ABD molecules were in hydrogen-bonded states on the naked Au surface. In the higher frequency region, three large absorption bands centered at 2960, 2928 and 2855 cm^{-1} are observed, which are attributed to the asymmetric stretching vibration of CH_3, and the asymmetric and symmetric stretching of CH_2, respectively. Special attention is paid on the asymmetric stretching peak of CH_2 (2928 cm^{-1}). Earlier spectroscopic studies done by Snyder et al. [43, 44] have demonstrated that the peak position of CH_2 stretching mode is a sensitive indicator of the packing degree of polymethylene chains. For example, in the crystalline polymethylene chains, the peak appears at 2920 cm^{-1}. An increase of this stretching mode (typically 4 – 8 cm^{-1}) usually implies a disordered structure. Since the ABD molecule has a large azobenzene chromophore, a direct comparison on the peak position of CH_2 stretching may be not so convincing. However the CH_2 stretching mode showed the largest peak shift on the naked gold surface as compared with all the SAM-modified substrates (see Table 1), suggesting that the ABD monolayer has the most disordered structure in this case.

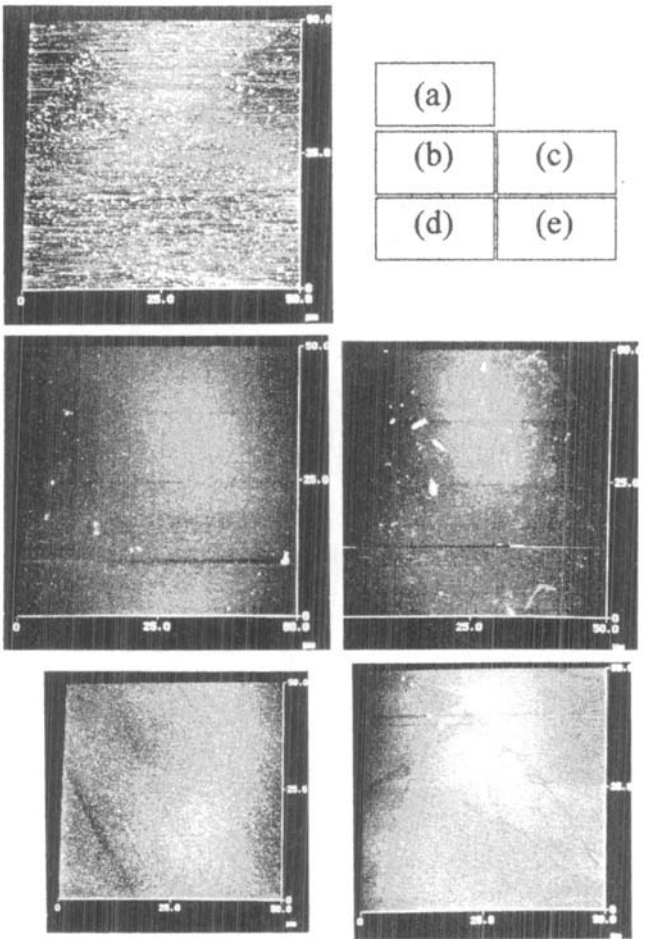

Fig. 3
50 × 50 μm AFM images of ABD LB monolayer on differently-modified gold substrates taken one day after LB deposition. (a) On naked Au; (b) Au/-COOH/HOOC-; (c) Au/-OH/HOOC-; (d) Au/-NH_2/HOOC-; (e) Au/-CH_2SO_3Na/HOOC-

With the above AFM and FTIR data, it is reasonable to say that ABD molecules have spontaneously rearranged in surface normal direction and the monolayer film structure has broken on the gold substrate. In fact, similar rearrangement phenomenon of LB film on naked gold has also been reported by J. L. Dote et al. [31]. They studied the infrared reflectance-absorption spectra (IRAS) of stearic acid monolayers on gold and found that the molecules in LB monolayer tend to rearrange into a three-dimensional structure with time aging. The structural instability we observed is believed to result from weak interaction between Au substrate and ABD molecules. The weak van de Waals interactions between them are not strong enough to prevent ABD molecules from three-dimensional rearrangement.

B(2). Au/-COOH/HOOC-

Inter-molecular interaction between the surface group -COOH of β-mercaptopropionic acid and the HOOC-group of ABD is expected to create hydrogen bond at the SAM/LB interface. The RA-FTIR spectra shown in Fig. 2b confirmed this expectation. Generally, the carboxylic acid group, -COOH, may exist in three different states: free monomeric state (-COOH), carboxylate state ($-COO^-$) and hydrogen-bonding dimer state, depending on the surrounding ambient [32, 33]. Each state gives a characteristic IR spectral band as mentioned above. In Fig. 2b, the hydrogen-bonded -COOH band is clearly seen at 1713 cm^{-1}. However, no spectral evidence was obtained for the presence of free -COOH, typically appearing around 1740 cm^{-1} [24], and for the presence of $-COO^-$, the antisymmetric and symmetric stretching modes of which should appear around 1550 and 1394 cm^{-1}, respectively [33]. This strongly suggests that the hydrogen-bonding dimer is the predominant structure at this SAM/LB interface. The schematic illustration shown in Fig. 4a may well explain the FTIR data, where two carboxylic acid groups create a most energetically stable eight-membered face-to-face hydrogen-bonding dimer. With such a face-to-face hydrogen-bonding configuration, the dipole moment of OH···O out-of-plane bending will be roughly parallel to the substrate surface, which was strongly supported by the distinctly weakened peak at 943 cm^{-1}.

B(3). Au/-OH/HOOC-

The RA-FTIR spectrum in this case is given in Fig. 2c. Similarly the strong spectral peak centered at 1707 cm^{-1} is attributed to the face-to-face hydrogen bonding between the surface -OH group and the HOOC- of ABD LB monolayer. It is noted that there is a remarkable shoulder in the high frequency side of the hydrogen-bonded carbonyl stretching band located at 1729 cm^{-1}. According to the works on similar monolayer assemblies by Smith [34] and Nuzzo [35], this shoulder should be assigned as a laterally-hydrogen-bonded carbonyl stretching vibration of two adjacent ABD molecules. This indicates that two different types of hydrogen bonding are existing at the Au/-OH/HOOC- interface: one is the vertical hydrogen bonding between SAM and LB layer and the other one is the lateral hydrogen bonding between ABD molecules in the same LB layer, as schematically shown in Fig. 4b.

B(4). Au/-NH_2/HOOC-

2-Amino-ethanethiol SAM-modified gold surface should be more easily positively-charged because its surface pK_b value was very small, 1.8 ± 0.2, as determined by contact-angle titration [36]. On the contrary, the carboxylic terminal group -COOH of ABD has a low pK_a value, suggesting its large proton-donating property. Therefore, proton transfer between the surface amino group, $-NH_2$ and the HOOC- group of ABD may occur, which leads to a coulombic attractive interaction at the SAM/LB interface. Fig. 2d shows the RA-FTIR spectrum of thus-designed interface. Comparing with the Au/-COOH/HOOC- and Au/-OH/HOOC- interfaces, the most remarkable spectral feature is the complete disappearance of both free acid carbonyl stretching band and hydrogen-bonded carbonyl stretching band. Instead, a number of new absorption peaks were observed at 2962, 1552 and 1390 cm^{-1}, which are assigned as NH_3^+ stretching, antisymmetric and symmetric stretching of $-COO^-$, respectively [33]. This strongly indicates the formation of ionic bond $-NH_3^+ {}^-OOC-$ at the SAM/LB interface as we expected. The antisymmetric and symmetric stretching bands of $-COO^-$ at 1552 and 1398 cm^{-1} are considerably weak, presumably due to the chemical environment of these vibrations. In Fig. 4c is given the schematic representation of the interfacial structure created in this case.

B(5). Au/-CH_2SO_3Na/HOOC-

The spectral feature of this interface is quite similar to the Au/-NH_2/HOOC- case as shown in Fig. 2e. No discernible absorption was observed at the spectral region of free and hydrogen-bonded carboxylic acid, suggesting the dissociation of proton from -COOH group. We also observed a new strong peak at 1058 cm^{-1}, which is attributed to the absorption of O=S=O group of $-SO_3H$. Therefore, it is reasonable to say that proton transfer has occurred at the Au/-SO_3Na/HOOC- interface. In addition, in spite of the weak intensity, we could also observe the antisymmetric and symmetric stretching modes of $-COO^-$ at 1552 and 1393 cm^{-1} [33], giving another evidence of the presence of $-COO^-$. The interfacial structure in this case is illustrated in Fig. 4d.

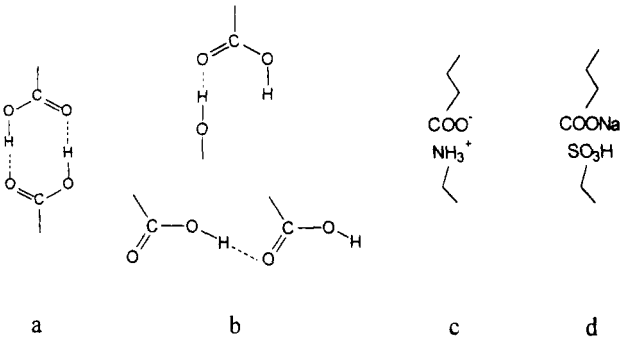

Fig. 4
Schematic illustration of the molecular bonding structures at differently-designed SAM/LB interfaces. (a) Au/-COOH/HOOC-; (b) Au/-OH/HOOC-; (c) Au/-NH_2/HOOC-; (d) Au/-CH_2SO_3Na/HOOC-

C. Stability

The stability of LB film structure is dominated by *molecule-molecule* interaction, *substrate-molecule* interaction, and their *relative strength* [37]. In the case of ABD monolayer on naked gold surface, the *molecule-molecule* interactions, including hydrophobic interaction between the long alkyl chains, aromatic interaction between azobenzene chromophores and hydrogen bonding between the carboxylic acid groups of ABD, are distinctly larger than the *substrate-molecule* interaction, which contains mainly the weak van de Waals interaction. This leads to the extremely poor stability observed. Actually, no more uniform film exists at all on the substrate surface because of the severe three-dimensional rearrangement. Modification of the gold surface using thiol SAMs improved the *substrate-molecule* interaction by introducing ionic bonding, hydrogen bonding, etc. These additional interactions are expected to improve the stability of ABD LB film on the gold surface.

C(1). In Air

Fig. 3b–e exhibits the 50×50 μm AFM images of ABD LB monolayer on different SAM-modified Au surfaces, obtained one day after preparation. Obviously, the morphological features of these SAM/LB composite films are completely different from that of ABD LB monolayer on naked Au (see Fig. 3a). All the films are shown to be quite uniformly distributed on the gold surface and less spots-like ABD aggregates were observed as compared with the Au/HOOC- case. This directly indicates that the SAM-modification of gold surface has effectively stabilized the monolayer structure and prevented the ABD molecules from destructive three-dimensional rearrangement. For comparison, we also took the AFM images of the SAM-modified Au substrates before deposition of ABD monolayer. All the

substrates showed uniform film morphology and no discernible difference was observed with four different SAMs. We noted that some granular structures are also seen occasionally in the AFM images of SAM/LB composite films. To identify the nature of these granules, the following preliminary μ-Raman experiment [38] was conducted: a ca. 2 μm laser spot ($\lambda_{ex} = 632.8$ nm) was focused on the individual granules, and Raman spectra in the $1100 - 1610\ cm^{-1}$ region were collected, most of which were typical of the spectra of azobenzene moiety of ABD [21]. The Raman intensity on the granules is much stronger than the surrounding, indicating the presence of very limited amount of ABD aggregates, probably occasionally occurred in the LB monolayer. Close examination of the AFM images revealed that the probability of such occasional molecular rearrangement seems to be dependent on the SAM terminal groups: the sequence was approximately Au/-OH/HOOC- > Au/-CH_2SO_3Na/HOOC- > Au/-COOH/HOOC- > Au/-NH_2/HOOC-, in which molecular rearrangement most easily occurred on the Au/-OH/HOOC- surface. This sequence is closely related to the stability of ABD monolayer on different SAM-modified gold surfaces, and can be well explained by the SAM/LB interfacial film structures derived from FTIR data. Considering the relative strength of SAM/LB interfacial bonding, the ionic bond formed at Au/-NH_2/HOOC- interface would be the strongest one, which tightly pinned the ABD molecules onto the substrate surface and thus effectively prevented their vertical rearrangement. In the case of Au/-COOH/HOOC-, the energetically favorate eight-membered hydrogen bonding can also effectively prohibit the destructive molecular rearrangement. Comparatively, the interaction between -OH and HOOC- would be the weakest one, which provided more possibility of occasional rearrangement. To our surprise, we got quite a uniform film with Au/-SO_3Na/HOOC- interface. At the present moment, the mechanism is still not clear, perhaps the negatively-charged -COO^- formed after deprotonation of carboxylic acid group inhibited the molecular rearrangement of ABD molecules. In addition, we noted that one day storage after LB film deposition from Langmuir trough is important to obtain stable AFM images. We imaged the composite films immediately after deposition and found that they were more easily damaged by the AFM tip scanning, which might be attributed to the presence of remnant water which made the film moved easily.

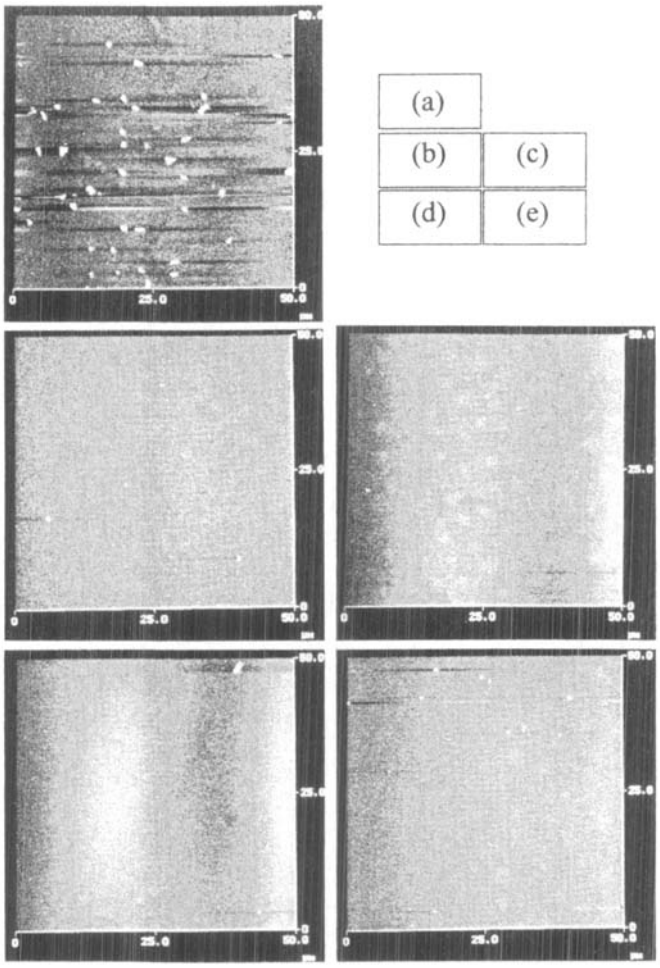

Fig. 5
AFM images of ABD LB monolayer on differently-modified gold substrates taken after 20-day time aging. (a) On naked Au; (b) Au/-COOH/HOOC-; (c) Au/-OH/HOOC-; (d) Au/-NH_2/HOOC-; (e) Au/-CH_2SO_3Na/HOOC-

To further testify the enhanced film stability, time aging experiment was done by monitoring the AFM morphology change with time. Fig. 5a – e shows the AFM images of Au/HOOC- and Au/-X/HOOC-, taken after 20-day storage in a desiccator at room temperature. As clearly seen from Fig. 5a, molecular rearrangement propagated more seriously on the unmodified gold surface and larger crystal-like granules were scattered over the substrate surface. Contrastively, on the SAM-modified gold surfaces, the uniform film morphology can still be clearly observed after 20-day time aging, indicative of the great enhancement of the long-term stability of ABD monolayer. The RA-FTIR measurements were also done on these time-aged films and no discernible changes were observed, consistent with the AFM results.

C(2). In Aqueous Solution

Actually one of the important motivations of designing the unique interfacial film structure using SAM technique is to study the long-range electron transfer kinetics across these differently-designed energy barriers, such as ionic bonding barrier, hydrogen bonding barrier, etc. For this reason, we investigated the stability of these SAM/LB composite films in aqueous solution. The electrochemical reactivity of azobenzene chromophore involved in ABD makes it possible to employ the conventional electrochemical approach for obtaining the stability information. Fig. 6 shows the cyclic voltammograms (CVs) of four different SAM/LB composite films, which were taken after extensive rinsing of the films using milli-Q water and after 1 min UV illumination. The UV illumination here was done for inducing the trans-to-cis photoisomerization of azobenzene chromophore in the composite films. The faradaic response ob-

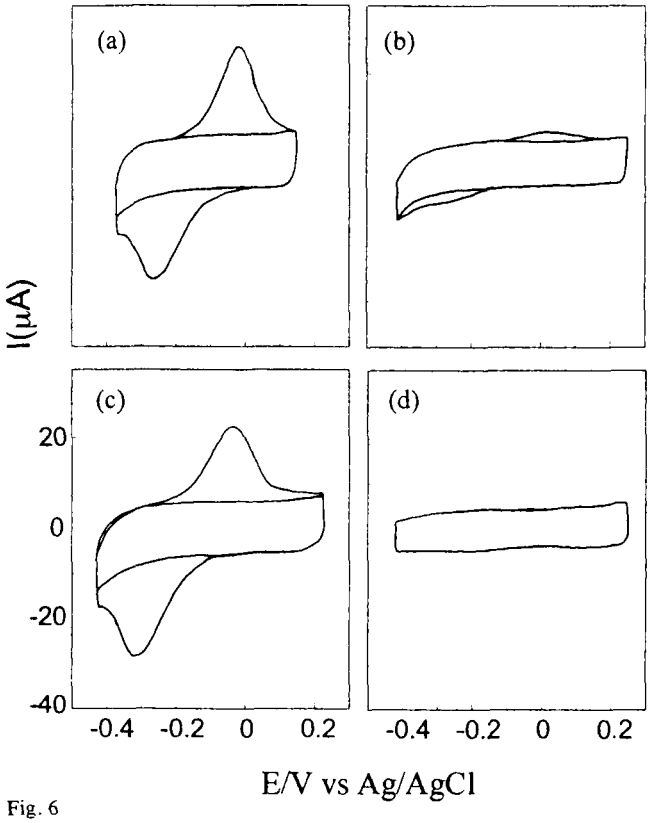

Fig. 6
Cyclic voltammetric responses of cis-azobenzene in different SAM/LB composite monolayer assemblies. The cis-azobenzene was obtained by 1 min UV irradiation of the film. (a) Au/-COOH/HOOC-; (b) Au/-OH/HOOC-; (c) Au/-NH_2/HOOC-; (d) Au/-CH_2SO_3Na/HOOC-. Scan rate: 200 mV/s; pH 6.0

tained was attributed to the electrochemical red-oxidation of the photoisomerization product, cis isomer of azobenzene chromophore [6, 7]. We have extensively investigated such photo-induced electrochemical responses of azobenzene monolayer assemblies in our previous publications [6, 7, 13–18]. Hence we will not go into the details here for confirming the formation of cis isomers under UV irradiation. Actually the photochromic property of azobenzene chromophore can be easily used for this purpose: immediately after UV irradiation, the composite film was exposed to 1 min visible illumination which can induce the reverse cis-to-trans photoisomerization, then the electrochemical response of cis isomers became almost disappeared; however, when irradiated with UV light again, the electrochemical response was recovered too; these operations could be excellently repeated, indicating that the reversible trans ⇔ cis photoisomerization has occurred in the composite films.

The Au/-COOH/HOOC- and Au/-NH_2/HOOC- exhibited the most stable CV properties, which did not show discernible change with water rinsing. In contrast, the CV of Au/-OH/HOOC- was not stable, and only small and varying faradaic responses were obtained after water rinsing. With Au/-CH_2SO_3Na/HOOC-, we could not observe any faradaic response at all. This observation agrees excellently with the RA-FTIR results obtained after water rinsing, as shown in Fig. 7. The rinsing brought about a remarkable change in IR spectra of Au/-OH/HOOC- and Au/-CH_2SO_3Na/HOOC-. In the former case, the shoulder observed at 1729 cm^{-1} in air, which was attributed to the laterally-hydrogen-bonded carbonyl stretching vibration of two adjacent ABD molecules, shifted to 1733 cm^{-1}, while the absorption band originating from the face-to-face hydrogen bonding between the surface -OH group and the HOOC- of ABD LB monolayer shifted from 1707 to 1704 cm^{-1}. Moreover, all the intensities of absorption bands showed a great decrease as compared to those obtained in air. These observations can be well understood supposing that the ABD molecules had been peeled off from the surface. On the other hand, in the case of Au/-SO_3Na/HOOC-, the spectral band characteristic of azobenzene chromophore completely disappeared. At the same time, the absorption peak of O=S=O group of -SO_3H shifted to a lower frequency, 1063 cm^{-1}, suggesting the formation of hydrated -SO_3H ions, and the water absorption band is clearly observed in the region of 1400 to 1800 cm^{-1}. In the high frequency region, all the absorption bands related to C-H stretching become remarkably decreased in intensity. All these results indicate that the ABD molecules have been almost completely dropped away from the -SO_3H- terminating substrate surface, in nice agreement with the absence of electrochemical reactivity.

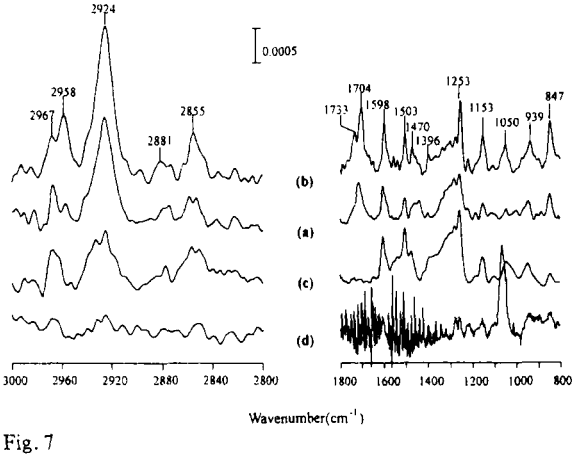

Fig. 7
RA-FTIR spectra of the SAM/LB monolayer assemblies after extensive water rinsing. (a) Au/-COOH/HOOC-; (b) Au/-OH/HOOC-; (c) Au/-NH_2/HOOC-; (d) Au/-CH_2SO_3Na/HOOC-

The above results give us two significant implications. Firstly, the stability of highly-organized LB film strongly depends on the surface physicochemical properties of supporting substrate. Secondly, one can effectively improve the structural stability of LB films through molecular level designing of the substrate surface.

Summary and Conclusion

We have designed a series of unique gold surfaces which are terminated by different functional groups by employing molecular self-assembling technique. These functionalized

substrates were used for deposition of azobenzene Langmuir-Blodgett monolayers. With infrared spectroscopic investigations, we confirmed that specific bonding has been created at the SAM/LB interface for each case. For instance, in the case of -COOH-terminated gold surface, the ABD monolayer is linked to the surface by an energetically stable eight-membered face-to-face hydrogen bond. Similarly hydrogen-bonded characteristic is also obtained at the Au/-OH/HOOC- interface though it is not as stable as the Au/-COOH/HOOC- case. On the other hand, proton exchange between the ABD carboxylic acid group and the surface terminal group has occurred at the Au/-NH_2/HOOC- and Au/-CH_2SO_3Na/HOOC- interfaces, where the former created a strong ionic bonding interface. AFM studies show that the film stability has been greatly improved on all these specially-designed surfaces as compared with the LB film simply deposited on naked gold at the destructive three-dimensional molecular rearrangement has been effectively prohibited. Our work demonstrates that the stability of highly-organized LB films strongly depends on the surface properties of the supporting substrates. Thus, one can stabilize the structures of the ordered films through molecular level designing of the substrate surfaces.

We gratefully acknowledge the State Science and Technology Committee, the State Education Committee and the National Natural Science Foundation of China (NSFC) for the financial support of this research. We also acknowledge Dr. Jiang Zhao for the helpful discussion on FTIR data.

References

[1] A. Ulman, An Introduction to Ultrathin Organic Films, Academic Press, Inc., New York, 1991.
[2] G.G. Roberts (ed) Langmuir-Blodgett Films, Plenum, New York, 1990.
[3] B. Michel, Highlights in Condensed Matter Physics and Future Prospects, p. 549–572, ed. by L. Esaki, Plenum, New York, 1991.
[4] Z.F. Liu, B.H. Loo, R. Baba, and A. Fujishima, Chem. Lett. 1023 (1990).
[5] Z.F. Liu, K. Hashimoto, and A. Fujishima, Chem. Lett. 2177 (1990).
[6] Z.F. Liu, B.H. Loo, K. Hashimoto, and A. Fujishima, J. Electroanal. Chem. *297*, 133 (1991).
[7] Z.F. Liu, K. Hashimoto, and A. Fujishima, J. Electroanal. Chem. *324*, 259 (1992).
[8] H.Z. Yu, Y.Q. Wang, S.M. Cai, and Z.F. Liu, J. Electroanal. Chem. *395*, 327 (1995).
[9] Z.F. Liu, C.X. Zhao, M. Tang, and S.M. Cai, J. Phys. Chem. *100*, 17337 (1996).
[10] H.Z. Yu, Y.Q. Wang, S.M. Cai, and Z.F. Liu, Langmuir *12*, 2843 (1996).
[11] Y.Q. Wang, H.Z. Yu, J.Z. Cheng, J.W. Zhao, S.M. Cai, and Z.F. Liu, Langmuir *12*, 5466 (1996).
[12] H.Z. Yu, Y.Q. Wang, S.M. Cai, and Z.F. Liu, Ber. Bunsenges. Phys. Chem. *101*, 257 (1997).
[13] Z.F. Liu, K. Hashimoto, and A. Fujishima, Nature *347*, 658 (1990).
[14] Z.F. Liu, K. Morigaki, K. Hashimoto, and A. Fujishima, Anal. Chem. *64*, 134 (1992).
[15] K. Morigaki, Z.F. Liu, K. Hashimoto, and A. Fujishima, Ber. Bunsenges. Phys. Chem. *97*, 860 (1993).
[16] K. Morigaki, Z.F. Liu, K. Hashimoto, and A. Fujishima, J. Phys. Chem. *99*, 14771 (1995).
[17] Z.F. Liu, K. Hashimoto, and A. Fujishima, Faraday Discuss. *94*, 1 (1992).
[18] Z.F. Liu, K. Morigaki, K. Hashimoto, and A. Fujishima, J. Phys. Chem. *96*, 1875 (1992).
[19] B.R. Herr and C.A. Mirkin, J. Am. Chem. Soc. *116*, 1157 (1994).
[20] W.B. Caldwell, K. Chen, B.R. Herr, C.A. Mirkin, J.C. Hulteen, and R.P.V. Duyne, Langmuir *10*, 4109 (1994).
[21] W.B. Caldwell, D.J. Campbell, K. Chen, B.R. Herr, C.A. Mirkin, A. Malik, M.K. Durbin, P. Dutta, and K.G. Huang, J. Am. Chem. Soc. *117*, 6071 (1995).
[22] Y.Q. Wang, J. Wang, H.Z. Yu, S.M. Cai, and Z.F. Liu, Chem. J. Chin. Univ. *17*, 1130 (1996).
[23] S. Hayashi and J. Umemura, J. Chem. Phys. *63*, 1732 (1975).
[24] S.E. Creager and C.M. Steiger, Langmuir *11*, 1852 (1995).
[25] R.G. Nuzzo, L.H. Dubois, and D.L. Allara, J. Am. Chem. Soc. *112*, 558 (1990).
[26] C.E.D. Chidsey and D.N. Loiacono, Langmuir *6*, 682 (1990).
[27] R.C. Duevel and R.M. Corn, Anal. Chem. *64*, 337 (1992).
[28] L. Sun, R.M. Crooks, and A.J. Ricco, Langmuir *9*, 1775 (1993).
[29] L. Sun, L.J. Kepley, and R.M. Crooks, Langmuir *8*, 2101 (1992).
[30] M. Zhang and M.R. Anderson, Langmuir *10*, 2807 (1994).
[31] J.L. Dote and R.L. Mowery, J. Phys. Chem. *92*, 1571 (1988).
[32] T. Kawai, J. Umemura, and T. Takenaka, Langmuir *5*, 1378 (1989).
[33] T. Kawai, J. Umemura, and T. Takenaka, Langmuir *6*, 672 (1990).
[34] E.L. Smith, C.A. Alves, J.W. Anderegg, M.D. Porter, and L.M. Siperko, Langmuir *8*, 2707 (1992).
[35] R.G. Nuzzo, L.H. Dubois, and D.L. Allara, J. Am. Chem. Soc. *112*, 558 (1990).
[36] H.Z. Yu, J.W. Zhao, Y.Q. Wang, J.Z. Cheng, S.M. Cai, and Z.F. Liu, Chem. J. Chin. Univ. *16*, 138 (1995).
[37] C.J. Miller, P. Cuendet, and M. Gratzel, J. Phys. Chem. *95*, 877 (1991).
[38] A Renishaw μ-Raman 1000 system equipped with a X-Y stage and a CCD detector was used in this experiment. A He-Ne laser (λ = 632.8 nm) was employed as the excitation light source. An optical microscope was used to position the focused light beam onto the desired region of sample surface. At the present we are also trying to map the sample surface using this μ-Raman system, thus we may directly compare it with AFM image.
[39] L.J. Bellamy, The Infrared Spectra of Complex Molecules, Wiley, New York, 1975, and Vol. II, Chapman and Hall, New York, 1980.
[40] D. Lin-Vien, N.B. Colthup, W.G. Fateley, and J.G. Grasselli, The Handbook of Infrared and Raman Characteristic Frequencies of Organic Molecules, Academic Press, Inc., 1991.
[41] M.D. Porter, T.B. Bright, D.L. Allara, and C.E.D. Chidsey, J. Am. Chem. Soc. *109*, 3559 (1987).
[42] Y.T. Tao, J. Am. Chem. Soc. *115*, 4350 (1993).
[43] R.G. Snyder, M. Maroncelli, H.L. Strauss, and C.A. Halknark, J. Phys. Chem. *90*, 5623 (1986).

(Received: March 4, 1997 E 9520
final version: May 15, 1997)